Graduate Research in Engineering and Technology (GRET)

Volume 1
Issue 4 *Emerging Aerospace Technologies in Aerodynamics, Propulsion, and Materials.*

Article 16

January 2022

Three-Dimensional Flow Analysis over Canard Configuration in Turbulence Model

L V S S Lohitasya Varun
Institute of Aeronautical Engineering, Dundigal, Hyderabad - 500043, varunllv16@gmail.com

Y. D. Dwivedi
Institute of Aeronautical Engineering, Dundigal, Hyderabad - 500043, yddwivedi@gmail.com

Recommended Citation
Varun, L V S S Lohitasya and Dwivedi, Y. D. (2022) "Three-Dimensional Flow Analysis over Canard Configuration in Turbulence Model," *Graduate Research in Engineering and Technology (GRET)*: Vol. 1 : Iss. 4 , Article 16.
DOI: 10.47893/GRET.2022.1061
Available at: https://www.interscience.in/gret/vol1/iss4/16

Three-Dimensional Flow Analysis over Canard Configuration in Turbulence Model

[1] *L V S S Lohitasya Varun,* [1] *Yagya Dutta Dwivedi*
[1] Department of Aeronautical Engineering, Institute of Aeronautical Engineering, Dundigal Hyderabad, Telangana, India – 500043.
Email: varunllv16@gmail.com

***Abstract* - The canard has been seen as an ominous aerodynamic object for ages this paper is to shed some more light on the effects of canard configuration on the aircraft's wings. This flow-field analysis is thus being done using a turbulence model solution to take into the effects of a real-time environment where the vortices from the canard are captured more accurately. The analysis has been done meticulously and made to be as error-free as possible under the guidance of Dr. Yagya Dutta Dwivedi.**

Keywords: Canard, Fluid Flow analysis, Turbulence analysis, K-Epsilon, Aeronautical, Vortex Capturing Method, Skin Friction Drag, Computational Fluid Dynamics.

I. INTRODUCTION

This computational analysis was performed to analyse and simulate the flow field around the canard equipped aircraft to better determine its aerodynamic characteristics and further improvise and implement necessary changes to bring it into the airline industry or at least the aeromodelling industry. The primary problem observed in the canard equipped aircrafts is that the stability of the aircraft has been greatly affected as the horizontal stabilizer is moved closer to the nose of the aircraft. This however can be overcome with present day technology with latest Autopilot Flight Control System. Thus, enabling us to overlook its disadvantages and reap the aerodynamic benefits that it has to offer. As most of the previous researches have shown that canard aircrafts have better aerodynamic efficiency [1] . The flow-field simulation is the primary concern of this research article where the pressure distribution, velocity gradients, streamline variation will all be observed and taken in for discussion based on the results obtained also while comparing the data so obtained from the previous research work where canard configured aircraft was used to experimentally determine the skin friction drag and also to capture the wake of the canard as well as the wing of the aircraft.

II. METHODOLOGY:

The motivation for the current research has been derived from the previous research works which depict the effects of canard configuration on the air flow around it. The inspiration for this work is the work done by Dr. Dwivedi [15] in which the skin friction drag was studied for a canard configuration, this is a continuation of his research to study the flow field in 3-Dimensional model using computational tools.

Generally, a major disadvantage of employing canard planes in aircraft is that the wake generated by the canard can affect the airflow over the main wing, resulting in a loss of lift.

Therefore, to overcome this issue, a high-wing, low-canard configuration was chosen for this study.

Airfoil Selection: Avistar airfoil [3] was chosen for the wing and Aquilasm airfoil [4] was chosen for the canard plane. The Aquilasm airfoil is great at low Reynold's number and more stable under turbulent flow conditions (generally used in turbines impellers). Similarly, the airfoil for the wing , Avistar which is a known airfoil in the RC aeromodelling community for its high lift at delayed stall angle enabling higher glide performance.

Preliminary analysis for the chosen airfoils was done using the X-Foil analysis tool available in XFLR V5 software as shown in Fig 1 and Fig 2

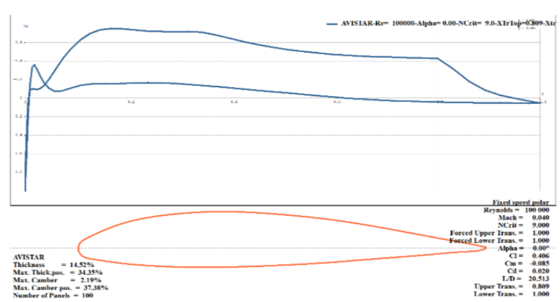

Figure 1:Avistar Airfoil with corresponding Cp graph

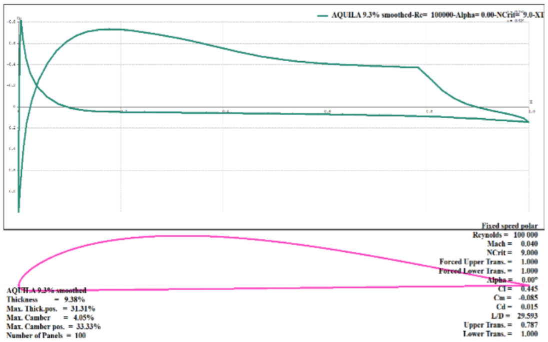

Figure 2: Aquilasm Airfoil with corresponding Cp graph

A. *Geometry Modelling*

The overall geometrical parameters for the wing, and canard, and the fuselage joining these two was taken from the work of (Dwivedi citation). The wing and canard were designed to have an aspect ratio 5 and 6 respectively so that the canard can stall before the wing reaches stall condition. The wing-span for the main wing is 0.4 meters. The main wing has a root chord of 0.087 meters and a tip chord of 0.07743 meters giving us a taper ratio of 0.89 because a taper wing produces smaller wingtip vortices than a rectangular wing and it also increases the aspect ratio thereby reducing induced drag and increases lift. The main wing also consists of a sweep back which is of 15 degrees as a sweep can further reduce drag.

The canard plane is a rectangular wing section having a chord length of 0.0375 meters throughout the span. The span of the canard plane is 0.225 meters. A fuselage was also designed having a total length of 0.3128 meters, width of 0.035 meters, and a height of 0.042 meters as shown in in Fig 3. Since, it is generally estimated that the fuselage length should ideally be between 75 and 80 percent of the wingspan. Hence, using this assumption, the fuselage length was assumed be 78.5% of the wingspan thereby giving us 0.3128 metres. Since this study focuses on the high-wing, low-canard configuration, the wing and canard were separated by 0.03 meters in such a way that the wing was placed 0.015 meters above fuselage reference line

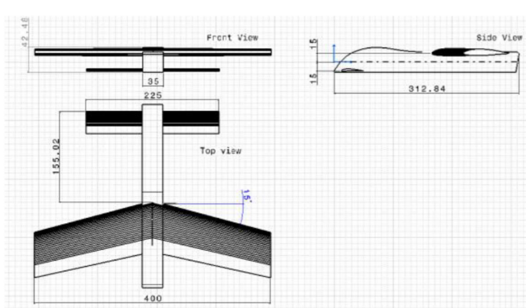

Figure 3: CAD Model with Dimensions

and the canard plane was positioned 0.015 meters below the fuselage reference line.

The 3D CAD modelling of the considered geometry was performed on CATIA V5 software (Fig-4). This geometry was further used for the computational analysis.

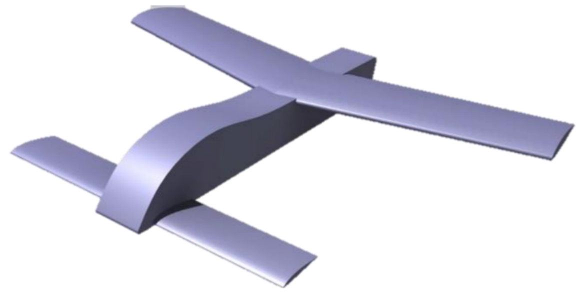

Figure 4: 3D Rendered CAD Model

TABLE 1 Canard Specifications

PARAMETER – CANARD	VALUE
AIRFOIL USED	Aquilasm
WINGSPAN	0.225m
CHORD LENGTH	0.0375m
ASPECT RATIO	6

TABLE 2 Wing Specifications

B. *Mesh Generation*

PARAMETER – WING	VALUE
AIRFOIL USED	Avistar
WINGSPAN	0.4m
ROOT CHORD	0.087m
TIP CHORD	0.077m
SWEEP	15^0
TAPER RATIO	0.89
ASPECT RATIO	5

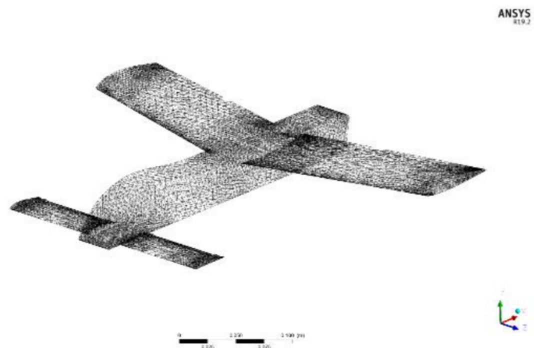

Figure 5: Aircraft Meshing

The mesh generated for the designed model has been generated with max mesh element sized at 14.027mm with inflation given near the canard and wings to better capture the flow characteristics near these structures as shown in Fig 5. The meshing metric was chosen to be Orthogonal Quality of the elements as this is one of the more widely accepted method to enhance the quality of the elements generated during meshing.

The inflation given to the aforementioned structures were given to be 5 layers with a growth rate of 1.2 between each layer. The assembly meshing of the model was done with tetrahedron elements. The outcome of which resulted in total of 42,25,990 elements and 7,33,352 nodes which is quite humongous for a moderately capable processor but the importance of the mesh quality precedented the

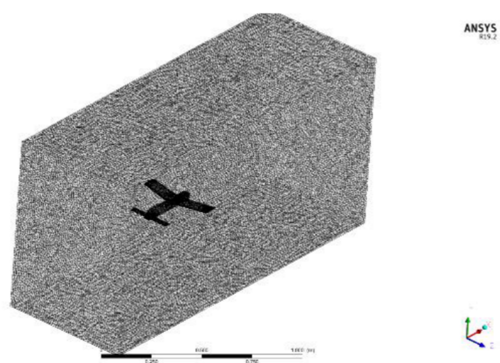

Figure 6: Entire Domain Meshing

processing time required to solve the analysis.

C. *Solver Settings*

The ANSYS FLUENT 19.2 workbench was used to solve the simulation using SIMPLE method with k-epsilon turbulent model which uses two equations. The Boundary Conditions were given for the model are specified in the Table 3.

BOUNDARY	TYPE	VALUE
INLET	Velocity – Inlet	30 ms^{-1}
OUTLET	Pressure - Outlet	Atmospheric
WALLS	No slip	NA

TABLE 3 Boundary Conditions

The convergence criteria was set to be 1e-04 and the convergence was observed to occur at around 430th iteration and the solution was stopped. The iterations were restricted to this number due to limited computational power of the processor.

Apart from the flow field analysis the lift and drag coefficient were also computed from this analysis and the results obtained were more than satisfactory when compared to Dr. Dwivedi's Experimental results. (Dwivedi , ICAB, et.al., 2019)

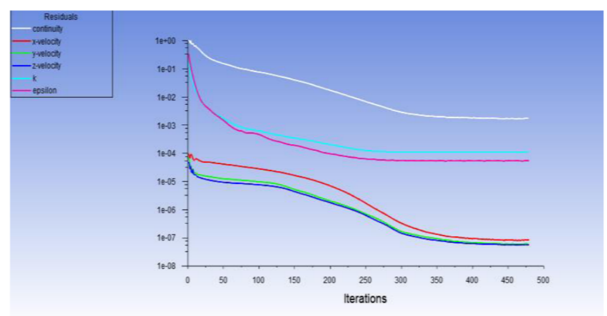

Figure 7: Convergence Plot

III. RESULTS AND DISCUSSION

The pressure and velocity contours were plotted for the simulated enclosure or domain constructed around the 3D model and results are as shown as below. The Local and Global Velocity contours are as shown in Fig 9 and Fig 10

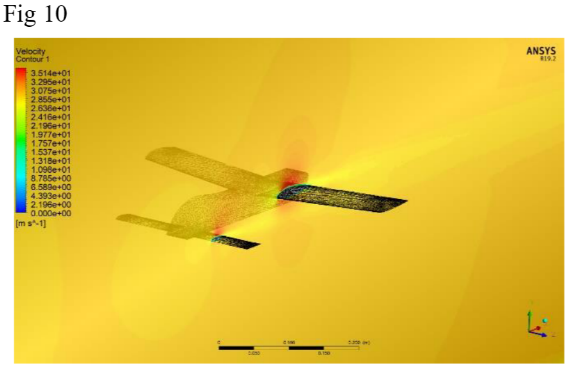

Figure 8: Local Velocity Contour

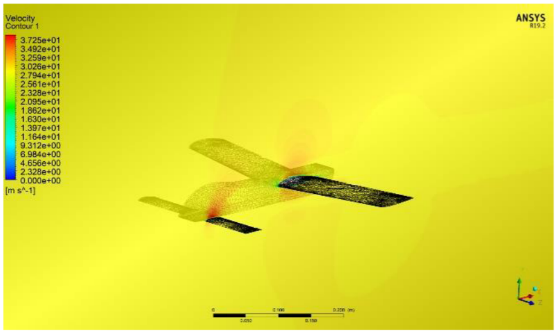

Figure 10: Global Velocity Contour

As it can be clearly observed the fluid(in this case air) is significantly being accelerated above the wing surfaces for both canard and the main wing but is zero on the surface of the aircraft with maximum and minimum velocities being 37.25ms^{-1} and 0ms^{-1} (On the surface of the body)

The resultant of which can be seen in the pressure contours below that shows the separation bubble with low pressure (blue/green bubble) at the top surface and high pressure (red/yellow bubble) at the bottom surface. The pressure contours demonstrate the boundary layer separation clearly at the middle of the airfoil cross-section where the bubble of separation dissipates as shown in Fig 10 and Fig 11. where maximum and minimum pressure were found to be 4.973e+02 Pa and -1.157e+03 Pa.

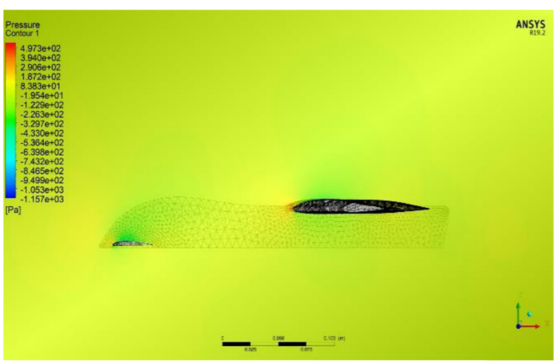

Figure 11: Global Pressure Contour

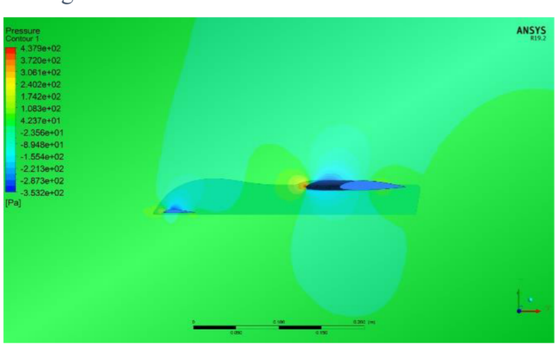

Figure 12: Local Pressure Contour

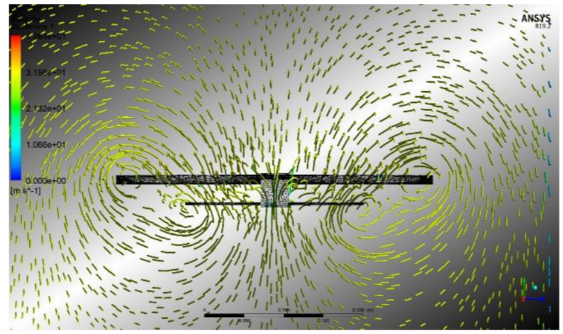

Figure 9: Vortex depicting Streamlines

The effective streamlines can be seen from the front view to capture the vortices formed at the tips of the wing and canard as shown in the Fig 12.
The captured vortices clearly show the rotation of the flow from higher pressure (lower side of the wing) to lower pressure (upper side of the wing)..
The obvious downside of the canard is that the wing must also face the advent of wing tip vortices from the canard but the low canard positioning enables that these vortices do not generate a wake in the wing's leading edge causing the wing to stall along its chord, which is technically impossible to recover from naturally.
The model was also simulated to observe the eddy viscosity along the wing surfaces which is depicted in the image below showing that the eddy viscosity is largely generated near the main wing where the fuselage and wing interfere and has negligible effect from canard. The flow domain was created large enough to capture all the contours and gradients properly without losing any important characteristic out of the box.

The eddy viscosity was observed to be a maximum of 3.171e-03 Pa-s and a minimum of 1.094e-05 Pa-s as shown in the Fig 13.

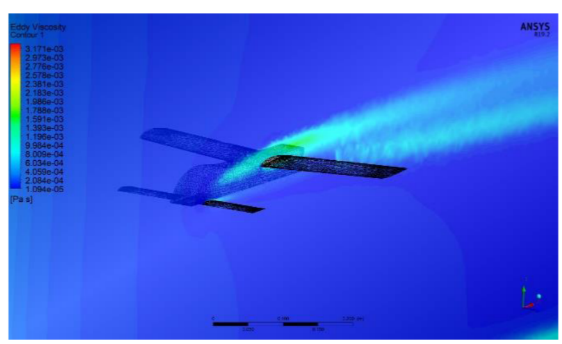

Figure 13: Eddy Viscosity Contours

IV. CONCLUSIONS

The computational fluid flow analysis was performed on the 3D designed model initially used to measure the skin friction drag on the same configuration. The model was simulated using ANSYS 19.2 FLUENT Workbench by developing the CAD Model using CATIA V5 and then importing the geometry into the FLUENT Workbench. The flow domain (enclosure) was approximately given with 3000mm in X-direction , 1500mm in Y-direction and 1000mm in Z-direction where all the distances are measured from the body of the aircraft called cushion distance. The entire aircraft body was subtracted (using Boolean) from the flow domain and treated as a wall which is conventional practice while performing CFD Analysis [5]. The entire domain was then meshed using tetrahedron elements with a maximum element size of 14.027mm using maximum orthogonal quality as the mesh metric for the grid generation.

The flow-field analysis can be said to be remarkably successful in achieving the results to match previous experimental works in the same configuration. The airfoil for the canard has been selected to be Aquilasm and Avistar airfoil has been selected for the main wing of the model.

- The wake at the trailing edge was visually captured from the both canard and the wing. The entire simulation was processed at 300,000 Reynolds Number using a k-epsilon turbulence model.
- The mesh was refined multiple times to enhance the capturing of the flow characteristics in close proximity to the model with great accuracy amounting the total mesh elements to be approximately 42 million elements.
- The canard produced a great amount of lift in addition to the wing.
- Although the canard too produces wing-tip vortices, The low canard and high wing configuration has significantly helped reduce this problem.
- The downwash from the canard has little to no effect on the aircraft. Anyways, this has also helped wing have a streamlined flow rather than turbulent flow directly attacking the leading edge of the wing.
- The flow-field has been successfully visualized computationally to verify the previous experimental research work done.
- All the parameters that were present during the wind-tunnel experiment have been exactly replicated in the computational model where applicable.
- The results of the experimental data have been successfully cross verified among other canard simulations

V. ACKNOWLEDGEMENT

Thanks to Dr. Dwivedi and his team for the basis of this research work.

Thanks to the ANSYS for providing license to their workbenches (ANSYS 19.2 FLUENT) without which, this paper wouldn't have been possible.

VI. REFERENCES

[1] Y. D. Dwivedi and L. Lohitasya Varun, "Aerodynamic Characterization of Albatross-Inspired Airfoils/Wings," *Int. J. Adv. Sci. Technol.*, vol. 29, no. 12s, pp. 801–815, May 2020, Accessed: Dec. 26, 2021. [Online]. Available: http://sersc.org/journals/index.php/IJAST/article/view/22543.

[2] P. Marques, A. Maligno, … S. D.-I. J. of, and undefined 2013, "Flight dynamics principles of canard aircraft: implications for UAV configuration decision," *search.proquest.com*, Accessed: Dec. 26, 2021. [Online]. Available: https://search.proquest.com/openview/1304bf1c9e949db35b2444ce7525b4ce/1?pq-origsite=gscholar&cbl=2032535.

[3] J. Ali, M. S.-J. of A. R. in Fluid, and undefined 2019, "Experimental and numerical study on the aerodynamics and stability characteristics of a canard aircraft," *akademiabaru.com*, vol. 53, pp. 165–174, 2019, Accessed: Dec. 26, 2021. [Online]. Available: https://www.akademiabaru.com/submit/index.php/arfmts/article/view/2420.

[4] E. T. Kim, Y. C. Kim, K. J. Seong, M. S. Hwang, and H. B. Eun, "A study on the parameter estimation for general aviation canard aircraft," *AIAA Atmos. Flight Mech. Conf. Exhib.*, 2003, doi: 10.2514/6.2003-5540.

[5] F. E. C. Culick, "Wright Brothers: First Aeronautical Engineers and Test Pilots," *AIAA J.*, vol. 41, no. 6, p. 4, 2001, doi: 10.2514/2.2046.

[6] B. P. Selberg and D. L. Cronin, *Aerodynamic-Structural Study of Canard Wing, Dual Wing, and Conventional Wing Systems for General Aviation Applications. University of Missouri-Rolla. Contract Report 172529*. National Aeronautics and Space Administration.

[7] A. K. Kundu, M. A. Price, and D. Riordan, *Conceptual Aircraft Design: An Industrial Approach*. John Wiley and Sons, 2019.

[8] Z. M. Ali, W. Kuntjoro, and W. Wisnoe, "Effect of canard to the aerodynamic characteristics of Blended Wing Body airplane," *ISBEIA 2012 - IEEE Symp. Business, Eng. Ind. Appl.*, pp. 696–700, 2012, doi: 10.1109/ISBEIA.2012.6422979.

[9] S. B. Wibowo, S. Sutrisno, and T. A. Rohmat, "The influence of canard position on aerodynamic characteristics of aircraft in delaying stall conditions," *AIP Conf. Proc.*, vol. 2021, p. 60028, Oct. 2018, doi: 10.1063/1.5062792.

[10] B. F. Ma, P. Q. Liu, and Y. Wei, "Effects of wing and canard sweep on lift enhancement of canard configurations," *J. Aircr.*, vol. 41, no. 6, pp. 1521–1523, 2004, doi: 10.2514/1.8707.

[11] J. Er-El and A. Seginer, "Vortex trajectories and breakdown on wing-canard configurations," *J. Aircr.*, vol. 22, no. 8, pp. 641–648, 1985, doi: 10.2514/3.45180.

[12] R. K. Singh, M. R. Ahmed, M. A. Zullah, and Y. H. Lee, "Design of a low Reynolds number airfoil for small horizontal axis wind turbines," *Renew. Energy*, vol. 42, pp. 66–76, Jun. 2012, doi: 10.1016/J.RENENE.2011.09.014.

[13] L. Q. Sang, J. Murata, M. Morimoto, Y. Kamada, T. Maeda, and Q. Li, "Experimental investigation of load fluctuation on horizontal axis wind turbine for extreme wind direction change," *J. Fluid Sci. Technol.*, vol. 12, no. 1, 2017, doi: 10.1299/JFST.2017JFST0005.

[14] R. E. M. Nasir, W. Kuntjoro, and W. Wisnoe, "Aerodynamic, Stability and Flying Quality Evaluation on a Small Blended Wing-body Aircraft with Canard Foreplanes," *Procedia Technol.*, vol. 15, pp. 783–791, Jan. 2014, doi: 10.1016/J.PROTCY.2014.09.051.

[15] *unpublished* Y. D Dwivedi and Nirmith Kumar Mishra et, al. "*Effect of Canard Vertical Locations on Skin Friction Drag of Sweep Wing Aircraft Model*" *ICAB Journal*